JMEPEG (2014) 23:3718–3726
DOI: 10.1007/s11665-014-1124-3

1059-9495/$19.00

Microstructure and Mechanical Properties of 316L Stainless Steel Filling Friction Stir-Welded Joints

L. Zhou, K. Nakata, T. Tsumura, H. Fujii, K. Ikeuchi, Y. Michishita, Y. Fujiya, and M. Morimoto

(Submitted May 25, 2013; in revised form December 25, 2013; published online June 27, 2014)

Keyhole left at 316L stainless steel friction stir welding/friction stir processing seam was repaired by filling friction stir welding (FFSW). Both metallurgical and mechanical bonding characteristics were obtained by the combined plastic deformation and flow between the consumable filling tool and the wall of the keyhole. Two ways based on the original conical and modified spherical keyholes, together with corresponding filling tools and process parameters were investigated. Microstructure and mechanical properties of 316L stainless steel FFSW joints were evaluated. The results showed that void defects existed at the bottom of the refilled original conical keyhole, while excellent bonding interface was obtained on the refilled modified spherical keyhole. The FFSW joint with defect-free interface obtained on the modified spherical keyhole fractured at the base metal side during the tensile test due to microstructural refinement and hardness increase in the refilled keyhole. Moreover, no σ phase but few Cr carbides were formed in the refilled zone, which would not result in obvious corrosion resistance degradation of 316L stainless steel.

Keywords austenitic stainless steel, filling friction stir welding, keyhole repairing, microstructure, mechanical properties

1. Introduction

With the increasingly severe resource and environment issues, nuclear power as a non-fossil energy is receiving more and more attention. However, absolute security must be guaranteed for nuclear power plants, otherwise disastrous accidents would occur and heavy loss would be caused. Austenitic stainless steel, AISI type 316 and its modified grades such as 316L, has applications as a structural material in nuclear power plants for the construction of water storage tanks. The choice of this alloy is based on its excellent high temperature tensile and creep fatigue strengths in combination with good fracture toughness and fabricability (Ref 1). However, there is an increasing incidence of stress corrosion cracking (SCC) problems in water storage tanks due to the continuous service of nuclear power plants around the world (Ref 2). The repair of SCC is becoming an urgent task to extend the service life of water storage tanks which have experienced SCC cracks at the external surface, and thus ensure the continued safety of nuclear power plants.

Friction stir processing (FSP) was first developed for superplasticity based on basic concept of friction stir welding (FSW) (Ref 3, 4), which has led to several applications including microstructural refinement/modification and surface/bulk composite preparation in metallic materials (Ref 5-7). The material in FSP zone undergoes extreme levels of plastic deformation and thermal exposure, which normally results in significant microstructural refinement and homogeneity of the processed zone, thereby improving strength, wear property, corrosion resistance among other properties. The technology of FSP also provides a high integrity smooth repair of internal or surface defects in structures formed in processes such as casting and welding. Compared with conventional fusion welding repair methods, this technology can offer advantages for online application particularly in terms of high joining quality and lower risk of through wall penetration. In our previous study, SCC on 316L stainless steel water storage tanks in nuclear power plants were repaired by FSP using polycrystalline cubic boron nitride (PCBN) tools (Ref 8, 9). However, a keyhole remains at the end of the seam inevitably, which would be the weakest part of the processed zone.

In a sense, the problems caused by the remaining keyhole can be solved by allowing the FSW tool to move onto a sacrificed run-off plate, but this method has its limitation. The auto-adjusting or retractable or double-acting FSW tools must be installed on exceedingly complex and expensive equipment. Furthermore, it is nearly impossible to realize a similar system for high melting point materials due to the limitations of pin tool materials and tool design (Ref 10-12). Refilling methods by fusion welding technology result in significant decrease of joint performance. Friction taper plug welding (FTPW) or friction hydro pillar processing (FHPP) is a solid state joining process developed by the welding institute (TWI) during the 1990s (Ref 13, 14), which involves drilling a tapered through hole or blind hole with very thin end wall into a plate and

L. Zhou, Joining and Welding Research Institute, Osaka University, 11-1 Mihogaoka, Ibaraki, Osaka 567-0047, Japan and Shandong Provincial Key Laboratory of Special Welding Technology, Harbin Institute of Technology at Weihai, Weihai 264209, China; **K. Nakata, T. Tsumura, H. Fujii,** and **K. Ikeuchi**, Joining and Welding Research Institute, Osaka University, 11-1 Mihogaoka, Ibaraki, Osaka 567-0047, Japan; **Y. Michishita** and **Y. Fujiya**, Manufacturing Technology Center, Mitsubishi Heavy Industries, Ltd., Takasago 676-8686, Japan; and **M. Morimoto**, Advanced Nuclear Plant Designing Section, Mitsubishi Heavy Industries, Ltd., Kobe 652-8585, Japan and ITER Superconducting Magnet Technology Group, Division of ITER Project, Japan Atomic Energy Agency, Naka 311-0193, Japan. Contact e-mail:zhouli_hit@163.com and zhouli@hitwh.edu.cn.

forcing the tapered rotating plug to the matching surface of the drilled hole to fix the defects in offshore steel and aerospace aluminum structures (Ref 15, 16). However, the preparation of a specific through hole or blind hole with very thin end wall for FTPW/FHPP is not desirable due to the limitations of the working environment and extra thick water storage tanks in nuclear power plants. Recently, a new technique called filling friction stir welding (FFSW) has been proposed by Huang et al., where a semi-consumable tool consists of non-consumable shoulder and consumable joining bit is used to repair the keyholes in aluminum alloy FSW welds without any changes to the keyhole shape (Ref 17, 18). However, it is much more difficult to fix the keyhole in high melting point materials, especially for stainless steel due to its high plasticization resistance and low thermal conductivity. In the present study, the remaining keyhole on the FSPed 316L stainless steel plates was repaired by FFSW using consumable tool with or without changing the original keyhole geometry. Microstructure and mechanical properties of FFSW joints were evaluated as a function of filling tool design and process parameters.

2. Experimental

The dimension of as-received 316L stainless steel plates was 200 mm × 150 mm × 10 mm and the filling tools were made of 316L stainless steel bar. The chemical composition and mechanical properties of the as-received plates and filling tools are shown in Table 1. The FSP process was performed using PCBN tool and the related details were given in previous publications (Ref 8, 9). The FFSW process was performed based on the original conical keyhole remaining after FSP and the modified spherical keyhole. The modified spherical keyhole was prepared by machining according to preliminary experiments, which is tangent with the contour of the original conical keyhole with the radius of 15 mm, as illustrated in Fig. 1(a). The corresponding filling tools were designed for the original conical keyhole and modified spherical keyhole, as shown in Fig. 1(b) and (c), respectively. The process conditions for FFSW were determined based on preparatory experiments, in which several welding parameters; the tool rotation speed (ω), applied force (*F*), and holding time (*T*), together with the filling

Table 1 Chemical compositions and mechanical properties of 316L stainless steel plates and filling tools

	Chemical compositions, mass%									Mechanical properties	
	C	Si	Mn	P	S	Ni	Cr	Mo	Fe	Tensile strength, MPa	Elongation, %
Plate	0.009	0.40	0.84	0.025	0.001	12.12	17.66	2.09	Bal.	558	59
Filling tool	0.015	0.24	1.67	0.036	0.012	12.02	16.71	2.00	Bal.	554	62

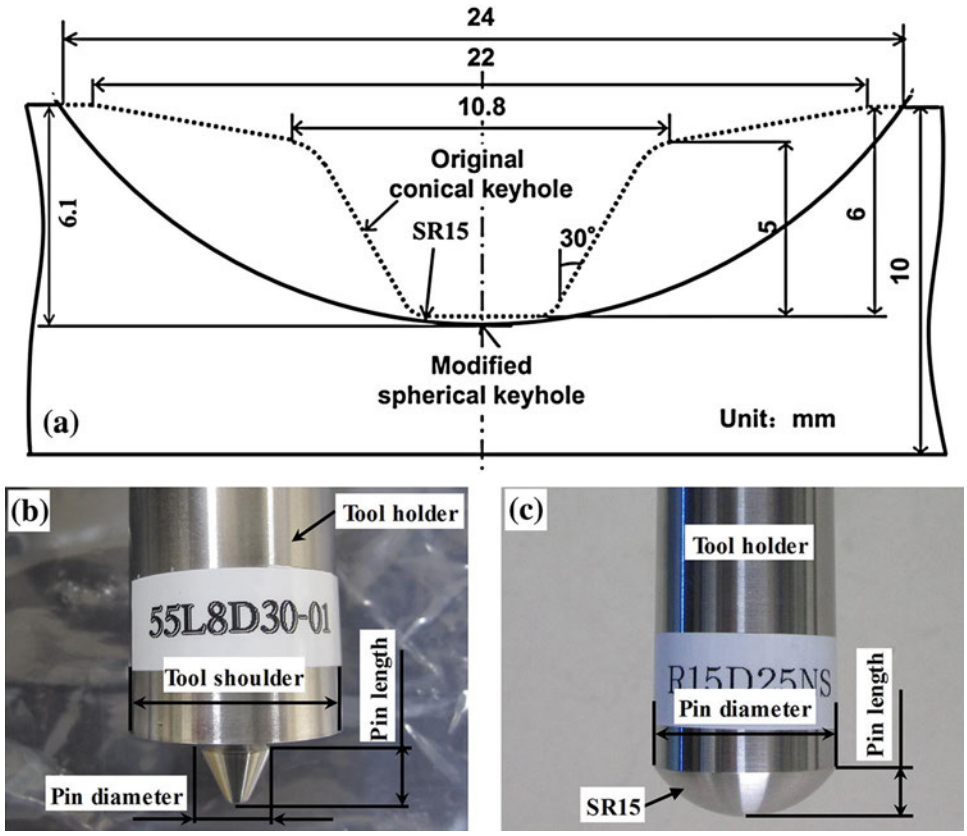

Fig. 1 Schematic illustration for FFSW process based on original conical keyhole and modified spherical keyhole: (a) illustration for original conical keyhole and modified spherical keyhole; (b) filling tool for original conical keyhole; and (c) filling tool for modified spherical keyhole

Table 2 Tool geometries and features for FSP and FFSW

Tool code	Tool geometry	Shoulder diameter, mm	Shoulder convex angle, °	Pin diameter, mm	Pin length, mm	Pin cone angle, °
FSP	Threaded conical pin	22	10	10.8	5	30
FFSW-conical	Smooth conical pin	24	15	9-13	8	50-60
FFSW-spherical	Smooth spherical pin	…	…	25	6.7	…

Table 3 Process parameters used for filling friction stir welding process

Tool code	Tool geometry	Applied force, kN	Tool rotation rate, rpm	Holding time, s
FFSW-conical	Smooth conical pin	35	1500	6, 9
FFSW-spherical	Smooth spherical pin	35	1500	6, 9

tool design were tried. Tool geometries and features for FSP and FFSW based on the original and modified keyhole are listed in Table 2. Hereinafter, the filling tools for the original conical keyhole are denoted as 50L8D30, 55L8D30, and 60L8D30 to stand for the tools with pin cone angle of 50°, 55°, and 60°, respectively. The tools used for the modified spherical keyhole are denoted as R15D25NS.

The FSP and FFSW process was performed on a load-controlled FSW machine with pure argon (≥99.99%) shielding employed around the welding zone to avoid surface oxidation. In common sense, relatively large applied force and tool rotation speed could result in more heat input to fully plasticize the material and get defect-free refilled joints. However, applied force and rotation speed are limited due to the operation in the water storage tank for nuclear power plants. In addition, the forging stage in conventional FTPW/FHPP process which supplies a large force without rotating the plug/tool as the final step also cannot be fulfilled in the system for practical application. In the present study, the applied force and tool rotation speed were kept constant at 35 kN and 1500 rpm (revolutions per minute), respectively. The varying holding time of 6 and 9 s together with tool design was investigated, as shown in Table 3. For the sake of brevity, the set of parameters are denoted as 35 kN-1500 rpm-6 s and 35 kN-1500 rpm-9 s hereinafter, respectively. During the welding, the actual value of process parameters was collected by data acquisition unit connected to the control system of FSW apparatus.

The refilled joints were examined by metallurgical inspections performed on the transverse cross-sections perpendicular to the original FSP direction and coincided with the central axis of keyhole. Microstructural evolution was examined by optical microscopy (OM; Keyence VHX-200/100F) and transmission electron microscopy (TEM; Hitachi HF2000). The transverse weld cross-sections were cut by electrical discharge machining and prepared by standard metallographic procedures. Samples were mounted in epoxy and ground with abrasive paper. Final polishing was conducted with 1 μm diamond paste abrasive. The polished joint cross-sections were electrolytically etched in a solution of 10% oxalic acid + 90% water with a power supply set to 15 V for 90 s, and then observed on the OM. TEM specimens were cut from the various locations of the joint cross-section using a focused ion beam instrument (SII SMI3050MS2) and were observed on the TEM at 200 kV. Vickers hardness along the transverse joint centerline was

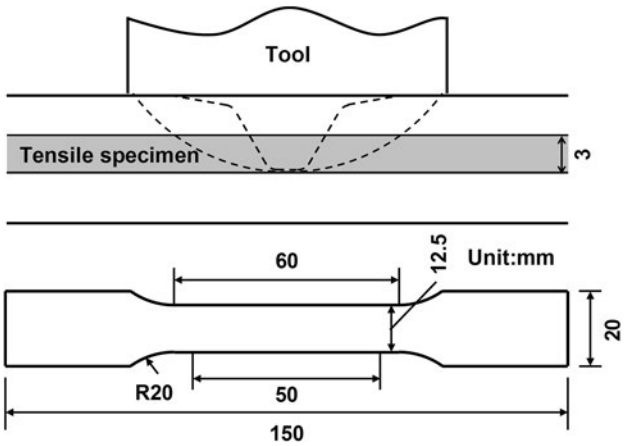

Fig. 2 Schematic illustration for tensile specimen of refilled joints

measured every 1 mm spacing at the position of 3 mm from the plate surface/bottom of RZ (center of the RZ along thickness direction) on an Akashi AAV-500 Vickers hardness tester using a load of 0.98 N for 15 s. Transverse tensile test samples with geometric details according to JIS Z2201 were cut perpendicularly from the bottom of the joint obtained under the same process conditions for metallurgical inspections with the top and bottom surfaces eliminated, as shown in Fig. 2 (Ref 19). Tensile tests were carried out on an Instron-5500 mechanical tester at room temperature with crosshead speed of 1 mm/min. The strain was measured using an extensometer based on a gauge length of 50 mm (Fig. 2).

3. Results and Discussion

Macroscopic overview of the cross-sections of refilled joint based on the original conical and modified spherical keyhole under different tool design and welding parameter are presented in Fig. 3. The typical refilled zone (RZ), base metal (BM), and the interface zone (IZ) in the refilled joints were observed, but no obvious heat-affected zone (HAZ) was formed due to the relatively low heat input and short high temperature dwell time. The joining condition at the IZ depends on the tool design and welding parameters. Some macro void defects (red frame) were

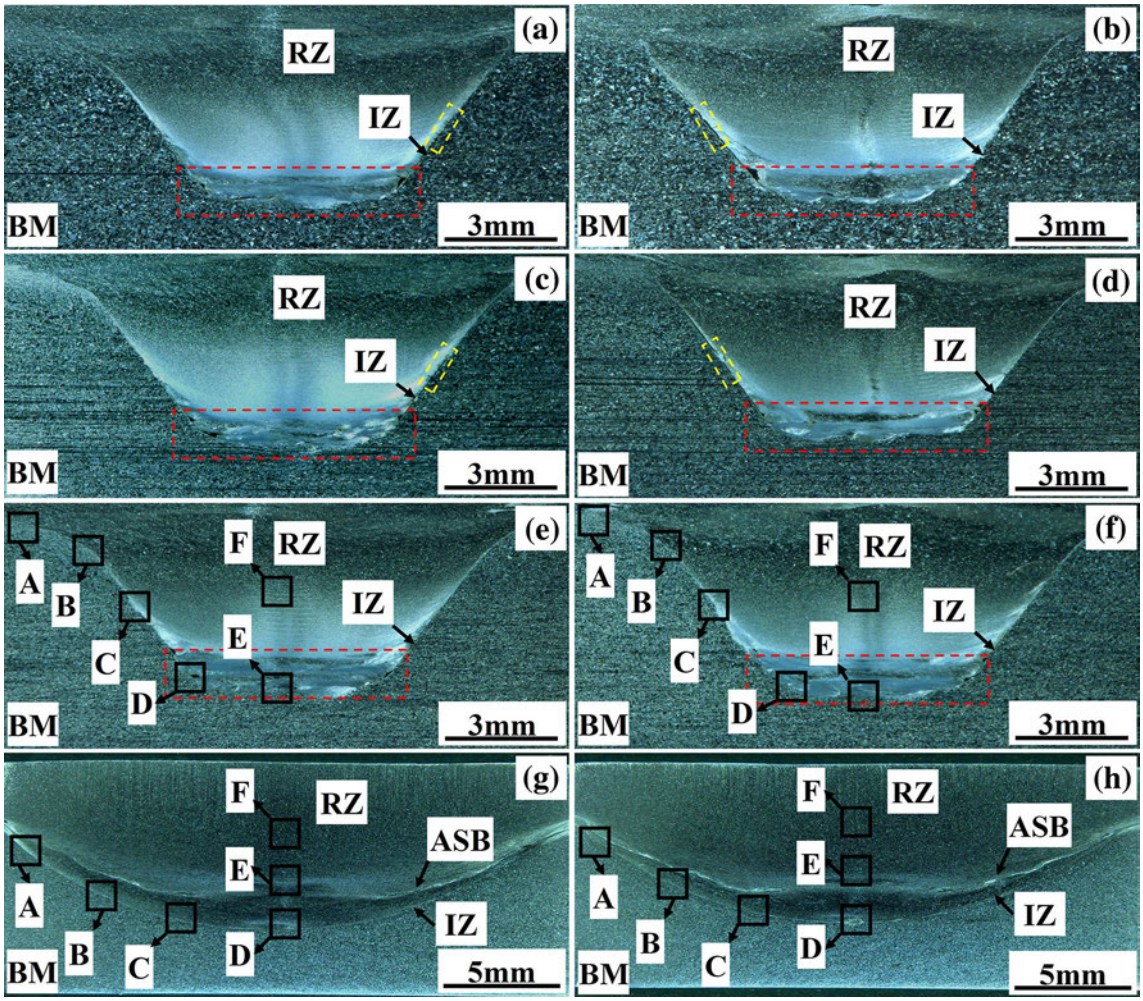

Fig. 3 Cross-section appearance of refilled original conical and modified spherical keyhole by FFSW with: (a) filling tool 50L8D30 under 35 kN-1500 rpm-6 s; (b) filling tool 50L8D30 under 35 kN-1500 rpm-9 s; (c) filling tool 55L8D30 under 35 kN-1500 rpm-6 s; (d) filling tool 55L8D30 under 35 kN-1500 rpm-9 s; (e) filling tool 60L8D30 under 35 kN-1500 rpm-6 s; (f) filling tool 60L8D30 under 35 kN-1500 rpm-9 s; (g) filling tool R15D25NS under 35 kN-1500 rpm-6 s; and (h) filling tool R15D25NS under 35 kN-1500 rpm-9 s

found at the bottom of the IZ in the refilled original conical keyhole under all the tool designs and welding parameters (Fig. 3a-f), while no obvious macro void defects were observed for that in the refilled modified spherical keyhole (Fig. 3g and h). In addition, non-bonding gaps (yellow frame) were found at the lower sidewall of the refilled original conical keyhole with filling tools 50L8D30 and 55L8D30 even under holding time of 9 s due to the excessive space between the keyhole and filling tool (Fig. 3a-d). With increasing pin cone angle and holding time, the condition at the lower sidewall of the refilled original conical keyhole could be improved, which is the case for the refilled joint by filling tool 60L8D30 under holding time of 9 s (Fig. 3e and f). As for the FFSW joints based on the original conical keyhole, arc-shape adiabatic shear layers (typical areas are denoted as position F in Fig. 3e and f) were formed in the RZ as that in conventional FTPW/FHPP joints due to continuous material plasticization (Ref 13, 14). However, no such obvious characteristics were developed in the RZ of FFSW joints for the modified spherical keyhole (Fig. 3g and h). However, it is interesting to note that an irregular lip-like adiabatic shear band (ASB) was formed in the RZ of the refilled modified spherical keyhole, which can be explained by the quite different thermo-mechanical effect and plastic deformation behavior as that in refilling the conical keyhole due to the difference in keyhole shape and filling tool geometry. In the current case, microstructural features in typical areas at the IZ and the RZ of the refilled joints (positions A-F shown in Fig. 3e-h) were mainly investigated. Microstructure in the base metal of the as-received plate and filling tool was also observed for comparison.

Microstructure of the base metal in the 316L stainless steel plates and filling tools are shown in Fig. 4, which consists of coarsened grain structures in the range of 30-80 μm distributed along the rolling/extrusion direction based on the linear intercept method (Ref 20). The details of the microstructural variations in typical positions of the FFSW joints based on the original conical keyhole using the filling tools 60L8D30 and modified spherical keyhole by filling tools R15D25NS are demonstrated in Fig. 5 and 6, respectively. As for the refilled original conical keyhole, it can be seen the upper part of the IZ was well bonded, as shown in Fig. 5(a)-(c). However, void defects were present at the bottom of the IZ regardless of the holding time, as indicated in Fig. 5(d) and (e). Microstructure image with high magnification for arc-shape adiabatic shear

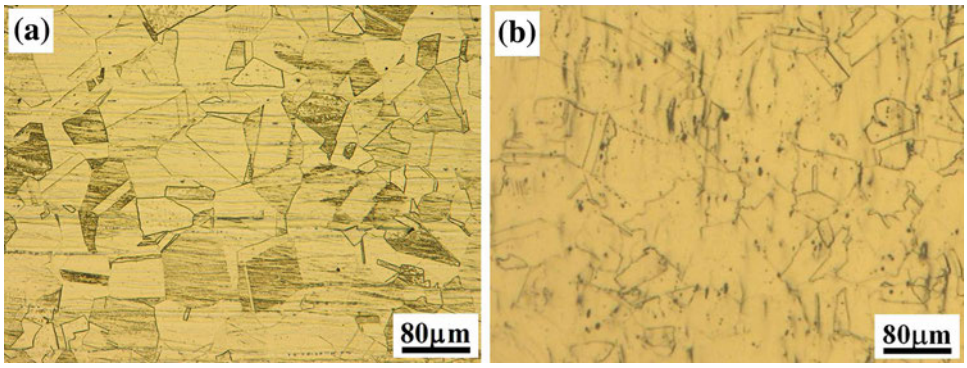

Fig. 4 OM microstructure of base metal in 316L stainless steel: (a) plates and (b) filling tools

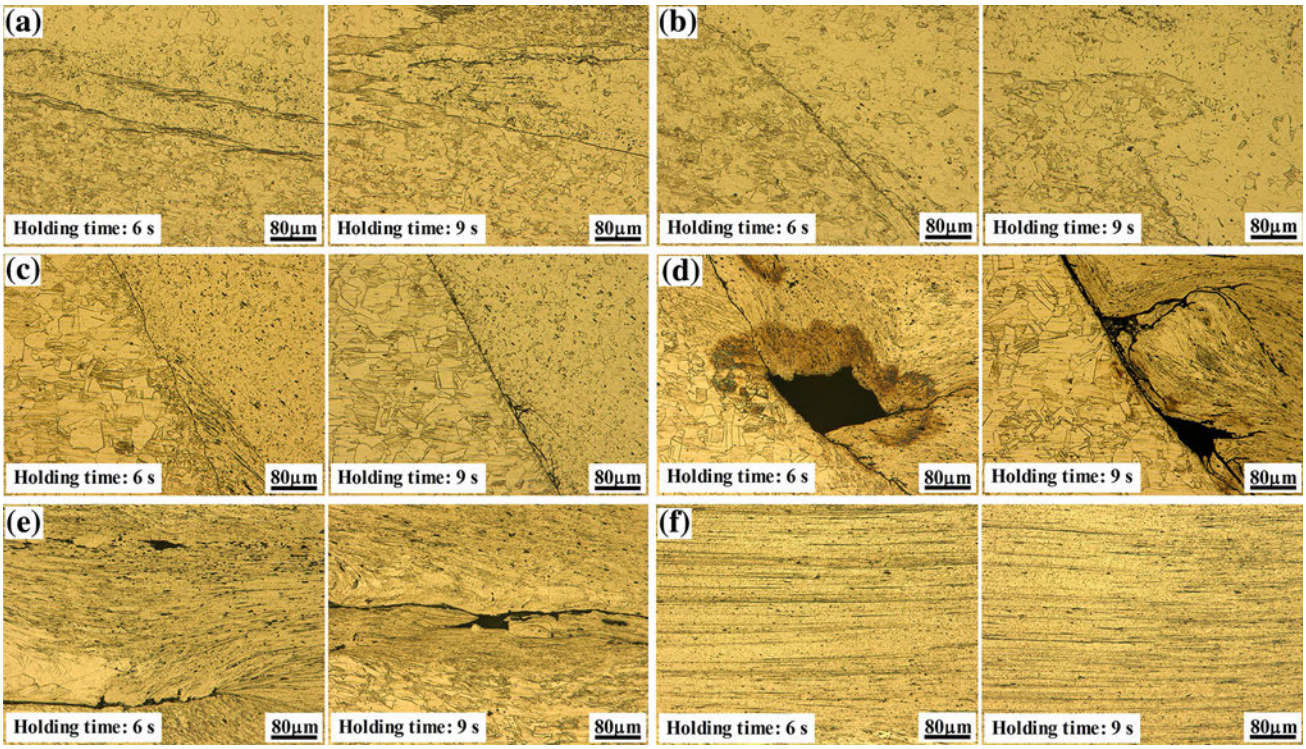

Fig. 5 Microstructure at different positions in refilled original conical keyhole shown in Fig. 3(e) and (f) by filling tools 60L8D30 under holding time of 6 and 9 s: (a) position A; (b) position B; (c) position C; (d) position D; (e) position E; and (f) position F

layers in the RZ of the refilled original conical keyhole indicates they consist of ultrafine DRXed grains of several microns, as shown in Fig. 5(f). In the case of the refilled modified spherical keyhole, non-bonding gap was formed in positions A and D at the IZ by the filling tool R15D25NS under the holding time of 6 s due to insufficient heat input and material plasticization, while the IZ was well bonded when the longer holding time of 9 s was adopted, as shown in Fig. 6(a)-(d). Grains in the IZ, especially the ones surrounding the keyhole surface, were significantly refined in all the refilled keyholes due to dynamic recrystallization (DRX) induced by severe plastic deformation during the process. Microstructure at the RZ in the refilled modified spherical keyhole is also characterized by refined grains, especially for the position at the ASB which endures even severe plastic deformation, as shown in Fig. 6(e) and (f). Furthermore, it is worth noting that besides the equiaxed DRXed grains, elongated deformed grains along the metal-flow direction were also present in all the FFSW joints due to the dynamic deformation process. It should be noted that black etch pits can be seen in the refilled keyholes, especially at the bottom of joint interface where the most serious deformation occurred and the grains were significantly refined, which could be explained by increased intergranular corrosion due to increase in grain boundaries caused by grain refinement. Moreover, the precipitation of little Cr carbides at the IZ which causes Cr depletion and results in the degradation of corrosion resistance of austenite stainless steel could be another reason, as will be discussed below (Ref 21).

Macro appearance and microstructure evolution in the refilled joints by FFSW is closely related to the thermal and mechanical effect exposed to the material, which can be revealed by typical process parameter graphs shown in Fig. 7. Process parameter graphs for the refilled original and modified keyholes obtained by filling tools of 60L8D30 and R15D25NS

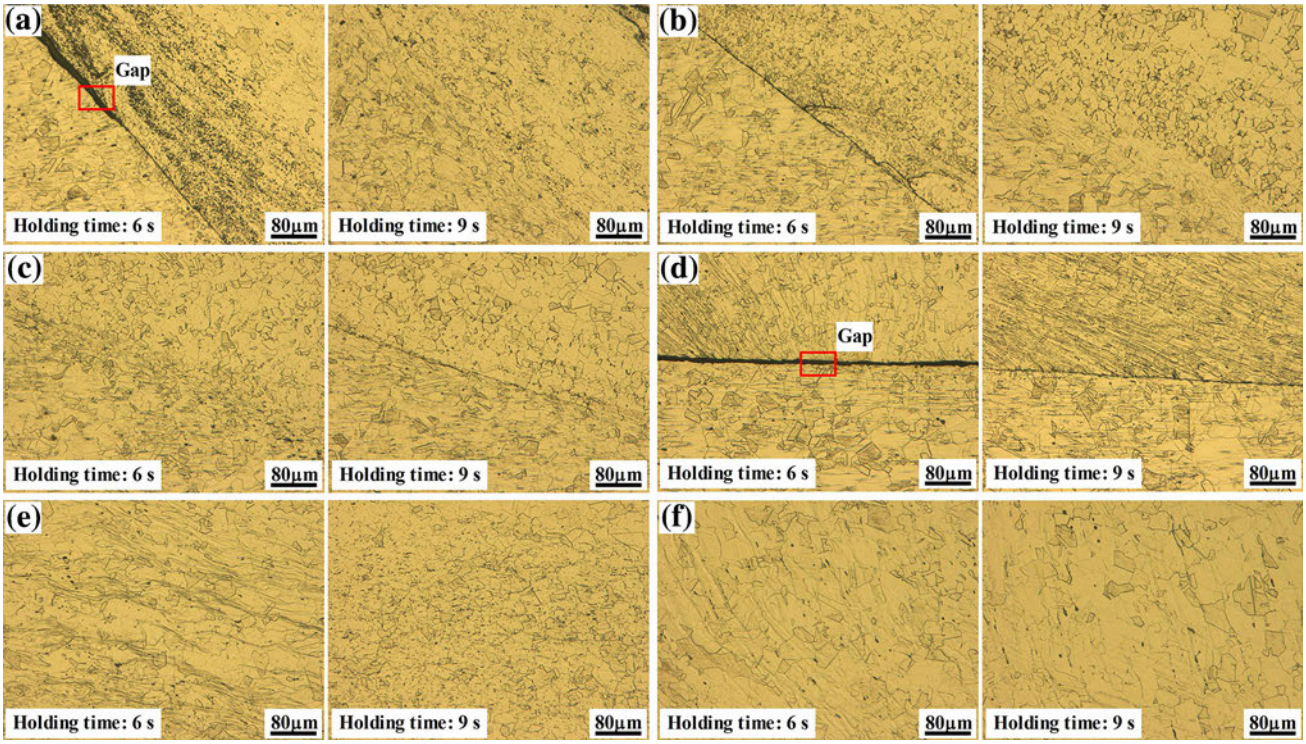

Fig. 6 Microstructure at different positions in refilled modified spherical keyhole shown in Fig. 3(g) and (h) by filling tools R15D25NS under holding time of 6 and 9 s: (a) position A; (b) position B; (c) position C; (d) position D; (e) position E; and (f) position F

under 35 kN-1500 rpm-9 s are shown in Fig. 7(a) and (b), respectively. It can be seen that the actual applied force increased to the set value of 35 kN quickly once the filling tool contacted with the keyhole and almost kept constant for applied holding time of 9 s at tool rotation speed of 1500 rpm. However, the tool torque during the refilling process for the above two cases for the original and modified keyhole was quite different due to the different keyhole/filling tool geometry and thermo-mechanical effect. For both cases, the tool torque reached to the peak value at the initial stage from the original value and descended due to the material plasticization. However, the peak value of tool torque during the refilling process for the original keyhole was much lower than that for the modified keyhole due to the smaller contact area between the keyhole and filling tool. Furthermore, the descending trend of tool torque for refilling the original keyhole was not so obvious as that for the modified keyhole after reaching the peak value (Fig. 7), which could be attributed to the deformation and contact with the keyhole of the conical filling tool shoulder (area A shown in Fig. 3f) though a convex angle was designed. In typical FTPW/FHPP process, the taper on the plug/hole did not exceed 30° to avoid the high axial thrust/applied force (Ref 13, 14). However, an applied force as high as 35 kN was needed for refilling the original conical and modified spherical keyholes due to the large taper and blind end for both cases, which led to the high reaction force and tool torque during the process. As for the original conical keyhole, void defects were formed at the bottom of the refilled joint due to the discontinuous plastic flow caused by the unsmooth geometry transition and small section modulus of the conical filling tool, especially under such high reaction force and tool torque. However, these problems could be avoided in the process for refilling the modified keyhole by spherical filling tool due to the smooth tool geometry transition and significantly increased tool section modulus.

Figure 8 shows the microhardness distributions, tensile properties, and fracture locations of the refilled joints with defect-free interface based on the modified spherical keyhole under process parameters of 35 kN-1500 rpm-9 s. It can be seen from Fig. 8(a) that the microhardness in the RZ is slightly higher than that of the base metal in the as-received plate (about 170 Hv), which could be attributed to microstructural refinement in the RZ of the refilled joint. The typical stress-strain curve showed a ductile fracture feature during the tensile test, and the corresponding tensile test sample did not fracture at the refilled keyhole but at the base metal side, as shown in Fig. 8(b). The tensile strength is evaluated by nominal stress and the elongation is determined by an extensometer based on the gauge length. The refilled joint consisted of base metal, RZ as well as interfaces between them. The observed tensile test result of refilled joint is general effect of these zones in the joints, and difference in tensile properties between the refilled joint and the as-received plate through the refilled joint was found though the refilled joint fractured at the base metal side. Tensile tests showed slight increase of the relative tensile strength and slight decrease of elongation in the refilled joint with defect-free interface for modified spherical keyhole (586 MPa and 54%, respectively) compared with that of the as-received plate (558 MPa and 59%, respectively). The refilled joints with defect-free interface for modified spherical keyhole fractured at the base metal side due to microstructural refinement and hardness increase in the RZ, and thus tensile strength which is the same level of that of the as-received plate was obtained. However, uniform elongation is lower due to the presence of the RZ with higher hardness in the refilled joints during the tensile test, which results in the decrease of

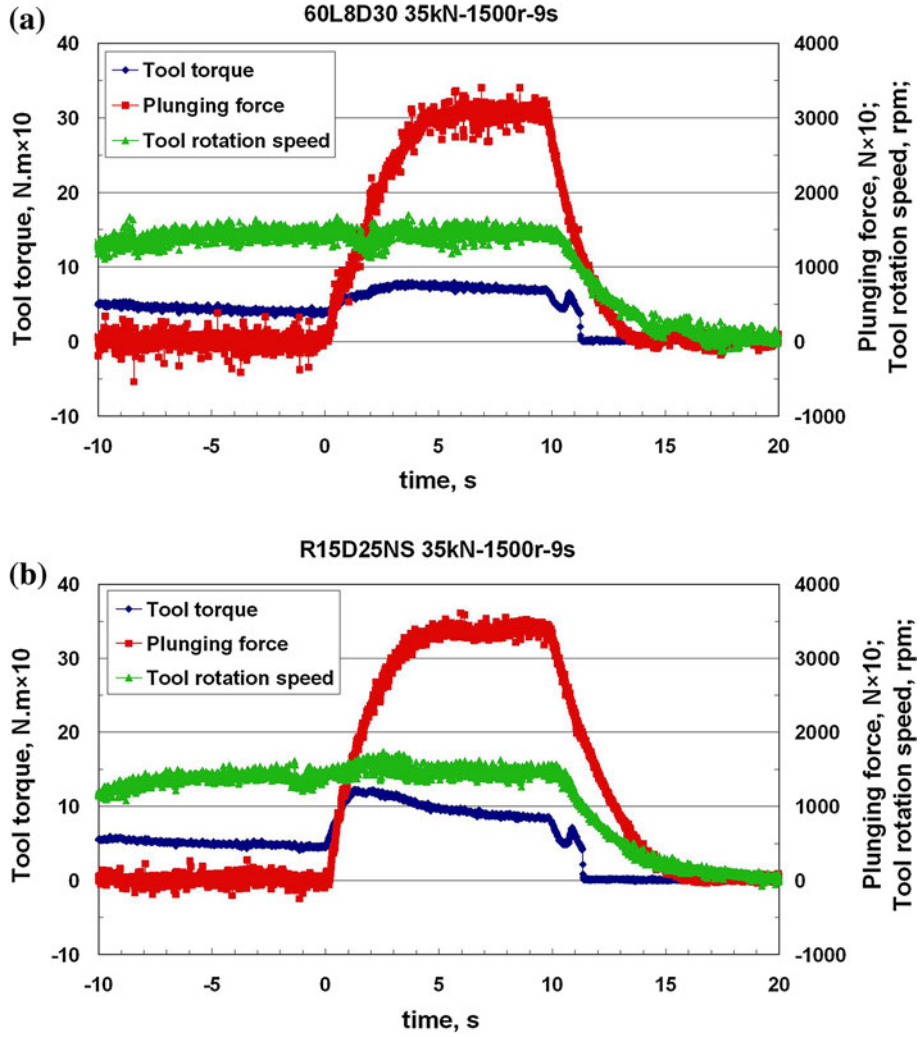

Fig. 7 Process graph for FFSW joints for (a) original conical keyhole using filling tool 60L8D30 under 35 kN-1500 rpm-9 s and (b) modified spherical keyhole using filling tool R15D25NS under 35 kN-1500 rpm-9 s

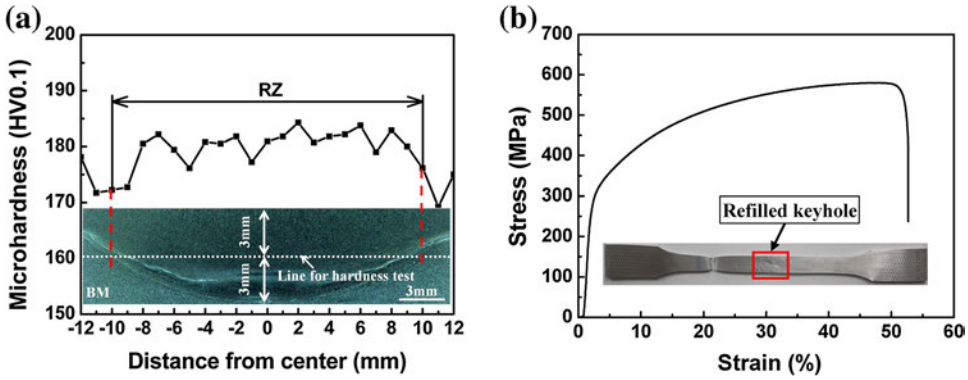

Fig. 8 Hardness profile and tensile properties of defected-free refilled joint by FFSW method on modified spherical keyhole by filling tool R15D25NS under 35 kN-1500 rpm-9 s: (a) microhardness distribution and (b) typical stress-strain curve and fracture location during tensile test

elongation compared with that of the as-received plate. The FFSW process for the modified spherical keyhole increases the effective bearing area of the joint, resulting in higher tensile strength, and thus is qualified for repairing the keyhole. Compared with previously proposed multi-step self-refilling friction stir welding (SRFSW) to refill the original conical keyhole using a series of specially designed polycrystalline cubic boron nitride (PCBN) tools (Ref 22), the present method

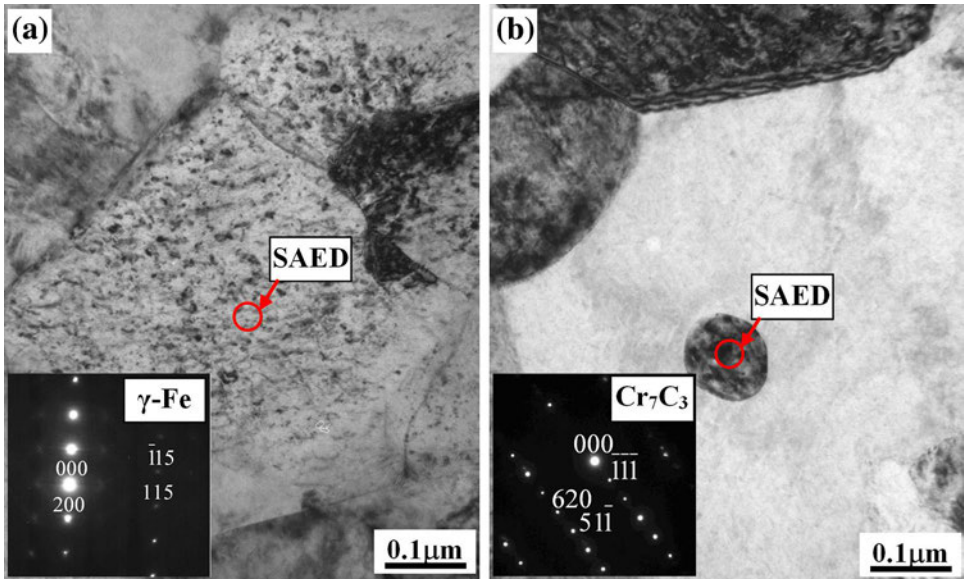

Fig. 9 TEM images of representative area (bottom part at the interface in refilled zone shown in Fig. 3: (a) austenite phase and (b) $Cr_{23}C_6$ phase

provides one-step solution using low-cost austenitic steel consumable filling tool despite the need to reshape the original keyhole and remove the excess filling tool material.

As for processes like FFSW based on the basic principles of FSW, the advantages result from the fact that the process takes place in the solid phase below the melting point of the material to be joined, especially for the materials that are difficult to be joined by conventional fusion welding method. As for austenitic stainless steel, σ phase, normally FeCr precipitates when exposed to elevated temperatures, which results in deleterious effect on toughness and ductility (Ref 23). Generally, σ phase is formed during aging at temperatures between 773 and 1073 K. In typical fusion welding process, the direct decomposition of austenite to σ phase requires long time due to the accompanying redistribution of alloying elements by substitutional diffusion (Ref 24). However, σ phase formation can be accelerated in the duplex microstructure of ferrite and austenite phases, especially by strain and recrystallization during aging (Ref 25, 26). Since FSW introduces high strain and it accompanies dynamic recrystallization in the stir zone, σ phase can be rapidly formed by the transformation of austenite to δ-ferrite at high temperatures and the subsequent decomposition of the ferrite under the high strain and recrystallization induced by friction stirring (Ref 8, 9, 27, 28). In our previous study for refilling the keyhole by SRFSW process, it has been verified that no σ phase, but very few Cr carbides were formed in the RZ due to the relatively short high temperature retention time compared with that in the conventional FSW/FSP process (Ref 22). As for the refilled joints based on the original or modified keyhole by the current FFSW process, microstructure in representative area (bottom part at the IZ) was further characterized by TEM, as shown in Fig. 9. No evidence of ferrite phase or sigma phase formation was identified, but austenite phase remained (Fig. 9a) and few rod-like types of carbide with the size of several hundreds of nanometers along the grain boundaries were observed. Carbides in austenitic stainless steel are of several types, which depend on metallurgical composition and process history. Generally, $Cr_{23}C_6$ is the most common Cr carbide in austenitic stainless steel and is given priority for formation during processing. In the present condition, the selected electron diffraction pattern for the typical positions of the IZ reveals that besides the $Cr_{23}C_6$ phase, the Cr_7C_3 phase with trigonal structure, a = 13.980 Å and c = 4.523 Å was also formed (Fig. 9b).

Compared with conventional fusion welding, the most attractive aspect for the FFSW process is that the base metal is not melted, and thus problems like porosity and grain boundary cracking associated with fusion welding repair technology can be eliminated and the mechanical property of the repair zone can be significantly improved. Moreover, it can offer advantages for online application particularly in terms of its lower risk of through wall penetration. Furthermore, the preparing a specific tapered through hole into a plate like that in the FTPW/FHPP process or the high-cost involved because of using a series of PCBN tools in the multi-step SRFSW could be avoided. The precipitation of Cr carbides could cause Cr depletion and result in the degradation of corrosion resistance of austenite stainless steel. However, the amount of Cr carbides in the RZ is very low and thus would not degrade the corrosion resistance of 316L stainless steel obviously due to the relatively short high temperature dwell time during the FFSW process. Therefore, FFSW technology to repair the keyhole is a promising online repair technology.

4. Conclusions

Keyholes in 316L stainless steel plates were repaired by filling friction stir welding technology using consumable tool based on the original conical keyhole and the modified spherical keyhole. The microstructure and the mechanical properties of the refilled joint were investigated. The important findings are summarized as follows:

(1) Void defects were formed at the bottom of the refilled original conical keyholes for all the tool design and

process parameters used, while the refilled joint with defect-free interface could be obtained on the modified spherical keyhole using corresponding filling tool under processing parameters set of 35 kN-1500 rpm-9 s. Microstructure surrounding the interface and in the refilled zone was significantly refined for all the refilled joints.

(2) The microhardness in the refilled zone of the refilled joint with defect-free interface on the modified spherical keyhole was slightly higher than that of as-received plate. Tensile test results showed the tensile specimen fractured at the base metal side of the refilled joint, and the relative tensile strength and elongation are 105 and 92% of the as-received plate, respectively.

(3) No σ phase but few Cr carbides were developed in the refilled keyhole due to the relatively short high temperature retention time. The precipitation of few Cr carbides would not cause obvious Cr depletion and result in the degradation of the corrosion resistance of 316L stainless steel.

Acknowledgments

The work was funded by the ''Innovative Nuclear Research and Development Program'' of the Ministry of Education, Culture, Sports, Science and Technology (MEXT), Japan.

References

1. K.H. Lo, C.H. Shek, and J.K.L. Lai, Recent Developments in Stainless Steels, *Mater. Sci. Eng. R*, 2009, **65**(4–6), p 39–104
2. C.W. Sun, R. Hui, W. Qu, and S. Yick, Progress in Corrosion Resistant Materials for Supercritical Water Reactors, *Corros. Sci.*, 2009, **51**(11), p 2508–2523
3. R.S. Mishra, M.W. Mahoney, S.X. McFadden, N.A. Mara, and A.K. Mukherjee, High Strain Rate Superplasticity in a Friction Stir Processed 7075 Al Alloy, *Scripta Mater.*, 1999, **42**(2), p 163–168
4. W.M. Thomas, E.D. Nicholas, J.C. NeedHam, M.G. Murch, P. Templesmith, and C.J. Dawes, Friction Stir Welding, GB Patent 9125978.8, Int Patent PCT/GB92/02203, 1991
5. R.S. Mishra and Z.Y. Ma, Friction Stir Welding and Processing, *Mater. Sci. Eng. R*, 2005, **50**, p 1–78
6. Z.Y. Ma, Friction Stir Processing Technology: A Review, *Metall. Mater. Trans. A*, 2008, **39**, p 642–658
7. Z.Y. Ma, A.L. Pilchak, M.C. Juhas, and J.C. Williams, Microstructural Refinement and Property Enhancement of Cast Light Alloys Via Friction Stir Processing, *Scripta Mater.*, 2008, **58**, p 361–366
8. Y.C. Chen, H. Fujii, T. Tsumura, Y. Kitagawa, K. Nakata, K. Ikeuchi, K. Matsubayashi, Y. Michishita, Y. Fujiya, and J. Katoh, Friction Stir Processing of 316L Stainless Steel Plate, *Sci. Technol. Weld. Join.*, 2009, **14**, p 197–201
9. Y.C. Chen, H. Fujii, T. Tsumura, Y. Kitagawa, K. Nakata, K. Ikeuchi, K. Matsubayashi, Y. Michishita, Y. Fujiya, and J. Katoh, Banded Structure and Its Distribution in Friction Stir Processing of 316L Austenitic Stainless Steel, *J. Nucl. Mater.*, 2012, **420**, p 497–500
10. R.J. Ding, and A. Oelgoetzp, The Hydraulic Controlled Auto-adjustable Pin Tool for Friction Stir Welding, US Patent No. 5893507, 1996
11. C.D. Allen, and W.J. Arbegast, *Evaluation of Friction Spot Welds in Aluminium Alloys*, SAE Technical Paper No. 2005-01-1252, SAE International, Warrendale, PA, USA, 2005
12. Y. Uematsu, K. Tokaji, Y. Tozaki, T. Kutita, and S. Murata, Effect of Re-filling Probe Hole on Tensile Failure and Fatigue Behavior of Friction Stir Spot Welded Joints in Al-Mg-Si Alloy, *Int. J. Fatigue*, 2008, **30**, p 1956–1966
13. S.B. Dunkerton, D.E. Nicholas, and P.D. Sketchley, Repairing Defective Metal Workpiece—By Friction Welding with a Metal Plug, Great Britain Patent Application No. 9125978, 1991
14. W.M. Thomas, and P. Temple-Smith, Friction Plug Extrusion for Solid-phase Welding Thick Plates—By Relatively Moving Consumable Member and Bore in Substrate while Urging Them Together to Generate Frictional Heat to Plasticize Member, Great Britain Patent Application No. 2306365, 1997
15. S.J. Unfried, M.T.P. Paes, T.F.C. Hermenegildo, F.L. Bastian, and A.J. Ramirez, Study of Microstructural Evolution of Friction Taper Plug Welded Joints of C-Mn Steels, *Sci. Technol. Weld. Join.*, 2010, **15**, p 506–513
16. P.J. Hartley, Friction Plug Weld Repair for the Space Shuttle External Tank, *Weld. Met. Fabr.*, 2002, **9**, p 6–8
17. Y.X. Huang, B. Han, Y. Tian, H.J. Liu, S.X. Lv, J.C. Feng, J.S. Leng, and Y. Li, New Technique of Filling Friction Stir Welding, *Sci. Technol. Weld. Join.*, 2011, **16**, p 497–501
18. Y.X. Huang, B. Han, S.X. Lv, J.C. Feng, H.J. Liu, J.S. Leng, and Y. Li, Interface Behaviors and Mechanical Properties of Filling Friction Stir Weld Joining AA 2219, *Sci. Technol. Weld. Join.*, 2012, **17**, p 225–230
19. Japanese Standards Association, Tensile Pieces for Tensile Test for Metallic Materials, JIS Z2201, 2004
20. ASTM International, Standard Test Methods for Determining Average Grain Size, ASTM E112-96, 2004
21. I. Woo, M. Aritoshi, and Y. Kikuchi, Metallurgical and Mechanical Properties of High Nitrogen Austenitic Stainless Steel Friction Welds, *ISIJ Int.*, 2002, **42**, p 401–406
22. L. Zhou, D. Liu, K. Nakata, T. Tsumura, H. Fujii, K. Ikeuchi, Y. Michishita, Y. Fujiya, and M. Morimoto, New Technique of Self-Refilling Friction Stir Welding to Repair Keyhole, *Sci. Technol. Weld. Join.*, 2012, **17**, p 649–655
23. J.C. Lippold and D.J. Kotecki, *Welding Metallurgy and Weldability of Stainless Steels*, Wiley Inc., Hoboken, 2005
24. M. Schwind, J. Kallqvist, J.O. Nilsson, J. Agren, and H.O. Andren, σ-Phase Precipitation in Stabilised Austenitic Stainless Steels, *Acta Mater.*, 2000, **48**, p 2473–2481
25. R.A. Farrar, Microstructure and Phase Transformations in Duplex 316 Submerged Arc Weld Metal, an Ageing Study at 700 °C, *J. Mater. Sci.*, 1985, **20**, p 4215–4231
26. Y.S. Sato and H. Kokawa, Preferential Precipitation Site of Sigma Phase in Duplex Stainless Steel Weld Metal, *Scripta Mater.*, 1999, **40**, p 659–663
27. S.H.C. Park, Y.S. Sato, H. Kokawa, K. Okamoto, S. Hirano, and M. Inagaki, Rapid Formation of the Sigma Phase in 304 Stainless Steel During Friction Stir Welding, *Scripta Mater.*, 2003, **49**, p 1175–1180
28. Y.S. Sato, N. Harayama, H. Kokawa, H. Inoue, Y. Tadokoro, and S. Tsuge, Evaluation of Microstructure and Properties in Friction Stir Welded Superaustenitic Stainless Steel, *Sci. Technol. Weld. Join.*, 2009, **14**, p 202–209